Macromolecular Symposia

www.ms-journal.de

Effect of Nitrogen Doping on Structural and Optical Properties of TiO_2 Nanoparticles

Sandip B. Deshmukh, Kalyani H. Deshmukh, Maheshkumar L. Mane, and Dhananjay V. Mane*

TiO_2 has materialized as an excellent heterogeneous photocatalyst for environmental and energy fields, including air and water splitting. It has 3.2 eV band gap with the absorption edge at near-UV light. Tuning of the band gap of TiO_2 into visible region is achieved by the doping of nitrogen. The optimum compositions of N doped TiO_2 NPs are prepared by sol-gel method at room temperature. The structural phase formation of materials is analyzed by XRD studies, which shows anatase phase. The crystallite size is calculated from XRD data, which is in nanometer range. FTIR spectra are studied to confirm the O-Ti-O, O-Ti-N bonding in N-doped TiO_2 and formation of -OH groups on the surface, which can extensively affect the TiO_2 band structure and surface of catalyst. The morphology of samples is investigated by FESEM and HR-TEM. The compositional stoichiometry is confirmed by EDAX analysis. An optical study is confirmed by UV-Visible spectrophotometer.

1. Introduction

The semiconducting metal oxide TiO_2 has been extensively employed as a photocatalyst owing to its high chemical stability, nontoxicity, cheap, good oxidation capacity, abundant, and, especially, excellent photocatalytic activity.[1,2] It has been proven that the desired photocatalytic properties of TiO_2 were achieved by fulfilling requirements in terms of high crystallinity, unique morphology, and mixed-phase composition, the potential of oxidizing and reducing under suitable irradiation.[3] Thus, because the band gap for the crystalline anatase phase TiO_2 is 3.2 eV with the absorption edge at near-UV light, when this semiconductor is exposed to near-UV light, the electrons in the valence band are excited to the conduction band produced an electron (e^-) and hole (h^+), generating a redox potential.[4,5]

A shift of the absorption band edge of TiO_2 toward the visible region can be achieved using several methods: the doping of TiO_2 with metals and non-metals, the sensitization of TiO_2 with dyes, the deposition of metals for localized surface plasmon resonance, and the amalgamation of TiO_2 with other semiconductors with a lower band gap. Another efficient method of developing visible light photocatalysts for the complete oxidation of volatile organic compounds is the modification of TiO_2 with uranyl ions.[6,7] In particular, visible light enhanced photocatalytic inactivation methods have been reported for the modification of TiO_2 with metals (e.g., iron, copper, vanadium, and tin) or nonmetals (e.g., nitrogen, sulfur, and boron). The most efficient approach to extend the photo response of titania into visible range is surface modification or doping with non-metals particularly.[8] N-doped TiO_2 has paying attention due to simple approaches to its synthesis and high photocatalytic activity under visible light. Di Valentin et al. [9] executed a computer simulation and showed that nitrogen impurities encourage the formation of localized energy states in the band gap of TiO_2. It was observed that N atoms substituted the lattice oxygen sites by mixing the N2p and O2p states.[10] These states lead to reduce the energy required to excite electrons and, consequently, to a red shift of the absorption edge.[11] The conventional solvothermal/hydrothermal methods are often energy and time consuming. Therefore, among these methods, the sol–gel method is commonly used for the synthesis of TiO_2-based materials due to its overruling advantages over others.[12]

In the present study, we report the N-doped TiO_2 NPs synthesized by the sol-gel method and the effect of N doping on structural and optical properties of TiO_2 NPs. We successfully obtained the anatase phase of N doped TiO_2 at low annealing temperature. The yields and product purity were remarkable.

2. Results and Discussion

2.1. X-ray Diffraction Analysis (XRD)

In order to evaluate the phase formation and crystalline structure of bare TiO_2 and various concentrations of N-doped TiO_2

S. B. Deshmukh, K. H. Deshmukh
Department of Chemistry
Ramkrishna Paramhansa Mahavidyalaya
Osmanabad, Maharashtra 413501, India
E-mail: sandipdeshmukh2244@gmail.com

M. L. Mane
Department of Physics
Shikshan Maharshi Guruvarya R. G. Shinde Mahavidyalaya
Paranda, Maharashtra 413502, India

D. V. Mane
Department of Chemistry
Shri Chhatrapati Shivaji Mahavidyalaya
Omerga, Maharashtra 413606, India

D. V. Mane
Yashwantrao Chavan Maharashtra Open University
Nashik, Maharashtra 422 222, India

The ORCID identification number(s) for the author(s) of this article can be found under https://doi.org/10.1002/masy.202100071

DOI: 10.1002/masy.202100071

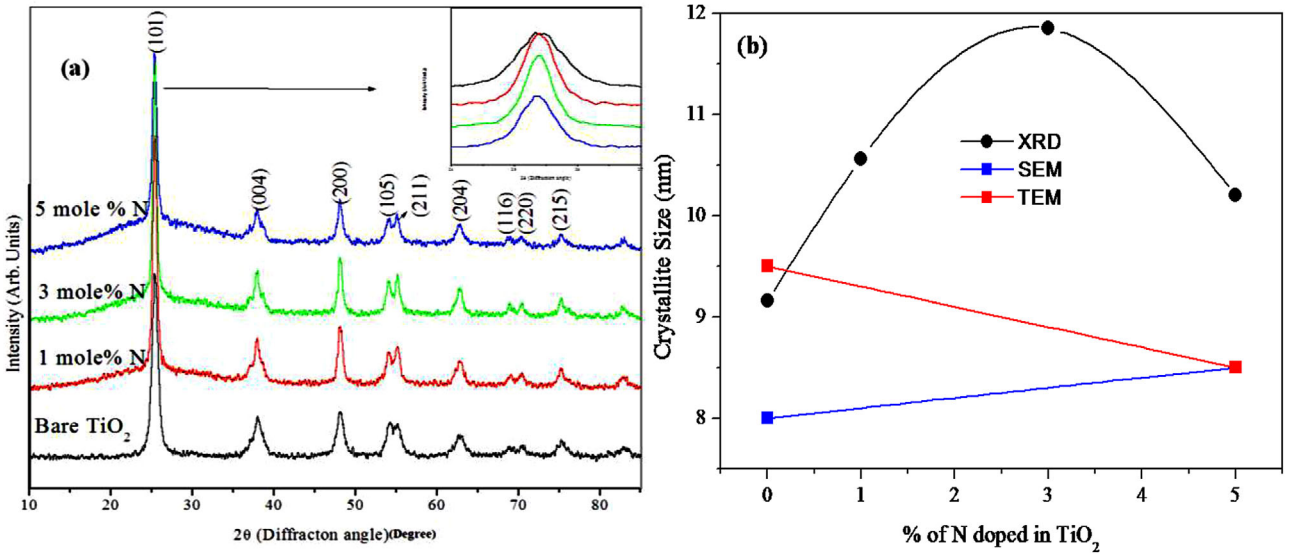

Figure 1. a) X-ray diffraction pattern for bare TiO_2 and N-doped TiO_2 NPs. b) Variation of crystallite size with % of N doped in TiO_2 NPs.

NPs, X-ray diffraction analysis was performed at room temperature using Cu-Kα radiations (λ = 1.5406 Å). **Figure 1**a shows XRD spectra of all the samples. The X-ray diffraction peaks (101), (004), (200), (105), (211), (204), (116), (220), and (215) of bare TiO_2 corresponding to diffraction angles at 2θ = 25.4°, 38.02°, 48.14°, 54.12°, 55.18°, 62.81°, 68.71°, 70.28°, and 75.30° could be attributed to the anatase phase TiO_2, respectively (JCPDS 21–1272).

No impurity phase was observed with N doping, the crystal structure of doped TiO_2 samples are almost unchanged when compared with that of bare TiO_2 sample. Also, it is observed that the peak positions of all diffraction peaks of N-doped TiO_2 samples are similar with those of pure TiO_2 NPs, however, a decrease in the anatase peak intensity was observed for (101) plane.[13] Furthermore, careful analyses of the main peak (101) of the anatase (inset, Figure 1a) indicated a slight shift to the higher angle side for N-doped TiO_2. The average crystallite size of all the samples was calculated from the Full Width at Half Maximum (FWHM) (β) of all major diffraction peaks of anatase, using the Debye-Scherer method.[14,15] The obtained results of the average crystallite size (D) before the doping was 9.10 nm and after the N doping it was changed as 10.55 , 11.85, and 10.21 nm for 1, 3, and 5 mole% of N. The variation of crystallite size with N mole% is shown in Figure 1b and it is observed that due to N doping crystallite size increases up to 3 mole % of N and further decreases for 5 mole% of N.

2.2. Fourier Transforms Infrared Spectroscopy (FTIR)

Figure 2 shows the FTIR spectra of bare TiO_2 and 1, 3, and 5 mole% N doped TiO_2. FTIR spectra was studied to confirm the O-Ti-O, O-Ti-N bonding in N-doped TiO_2 and formation of -OH groups on the surface, which can extensively affect the TiO_2 band structure and surface of photocatalyst. In the FTIR spectra absorption peaks in the range of 1365–1395 and 400–500 cm^{-1} demonstrate vibration of Ti-O bonding.[16] In all spectra, the

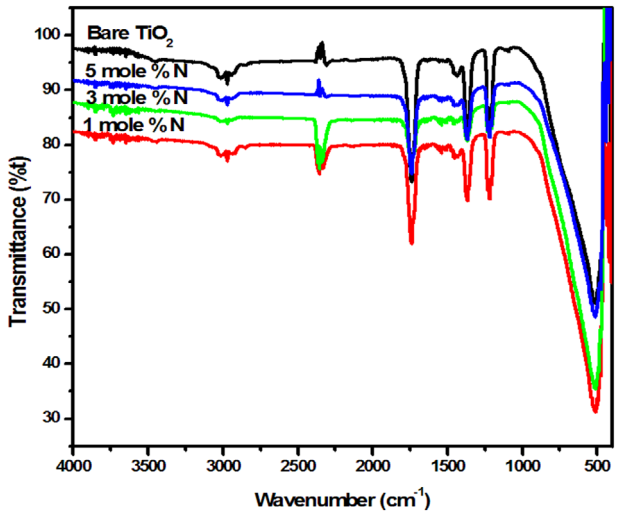

Figure 2. FTIR spectra of bare TiO_2 and N-doped TiO_2 NPs

strong absorption was observed in the range of 400–1250 cm^{-1} with a sharp peak at 488 cm^{-1}, which is attributed to the lattice vibrations of anatase O-Ti-O bonding in TiO_2. The weak band for bending vibrations of H-O-H bonds of the surface adsorbed water was observed at ~1612 and 1430 cm^{-1}.[17] N doping has been confirmed by the peaks at 1470 and 1270 cm^{-1}, which can be attributed to Ti-N and O-N vibration.[18] Besides, broad bands centered at around 3400 cm^{-1} show the presence of -OH groups.

2.3. Field Emission Scanning Electron Microscopy (FESEM)

In **Figure 3**a, b, and c, FESEM images show the surface morphology of bare TiO_2, 1% and 5 mole % N-doped TiO_2 synthesized by using sol-gel method and calcined at 500°C. It is evident from these images that the N-doped TiO_2 were included of non-spherical tiny particles with an average diameter of 7–10 nm

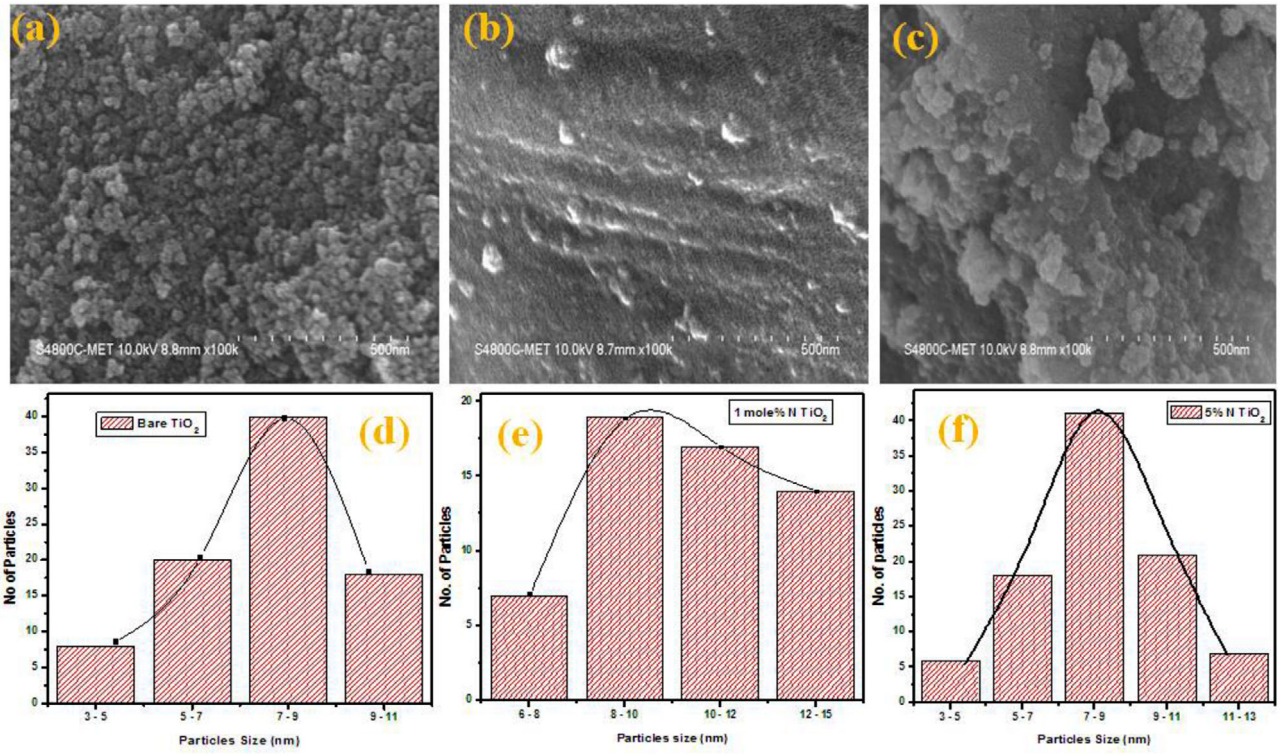

Figure 3. FESEM images of (a) bare TiO_2, (b) 1% N doped TiO_2, and (c) 5% N-doped TiO_2 and corresponding histograms of samples (d), (e), and (f).

of its particle size. The particle size of these samples was estimated by measuring the diameter of the particles from Gaussian fitting of histograms. Figure 3d–f represents the particle size distribution Gaussian fitting of histograms, and average particle size is determined. The histogram shows an average size distribution is 8.6 nm. The average particle size determined from Gaussian fitting is in close agreement with the particle size calculated from XRD analysis. The N-doped TiO_2 is compared with the bare TiO_2, the diameter and morphology did not change significantly because the amount of N-doped on TiO_2 was very less, so the TiO_2-doped of N in the SEM image is difficult to observe effectively.

2.4. Energy-dispersive X-ray Analysis (EDAX)

The elemental composition of N-doped TiO_2 spheres with varying amounts of N loading calcined at 500°C was analyzed using EDAX. EDAX was used to determine the elemental composition of the NPs and the representative patterns are shown in **Figure 4**a, b, and c. These patterns reveal the presence of Ti, N, O elements in the doped samples element. It can be observed that the intensity of the N peak corresponding to emission lines at 0.4 keV(Kα1) increases with increasing N doping by comparing the EDAX spectra of the N-doped samples with that of bare TiO_2. The presence of a 0.3, 0.4, 0.5, 0.6, 4.5, and 4.9 keV (Lα1) peaks are attributed to the Ti and O. In Figure 4a, only Ti and O elements were detected in bare TiO_2 powder, while in Figure 4(b) and (c), N was detected in addition to Ti and O elements in N-doped TiO_2, indicating that N was successfully doped on the TiO_2. Elemental composition of O (K), Ti (K), and N (L) in weight% for bare TiO_2 was 22.78, 77.22, and 0, for 1 mole% N was 17.11, 82.6, and 0.29 and for 5 mole % was 15.45, 83.2, and 1.35. Elemental composition of O (K), Ti (K), and N (L) in atomic% for bare TiO_2 was 46.90, 53.10, and 0, for 1 mole% N was 39.51, 60.13, and 0.36 and for 5 mole% N was 36.59, 62.02, and 1.39.

2.5. High-resolution Transmission Electron Microscopy (HR-TEM)

The surface morphology and particle structure of bare and 5 mole% N-doped TiO_2 NPs was analyzed by using HR-TEM technique. The representative HR-TEM images of the bare TiO_2 are shown in **Figure 5**a–d, which show the TEM, high-resolution TEM (HR-TEM), histogram of particle size, and selected area electron diffraction (SAED) pattern. These images confirm that the bare TiO_2 particles show a spherical-like structure with a size distribution from 9 to 11 nm. While images of N-doped TiO_2 shown in Figure 5e–h confirm that the 5 mole % N doped TiO_2 NPs are elongated-spherical in shape with an average size of 7–9 nm. The NPs are clearly observed in all the images, which shown the high degree of crystallinity. The particle size of 5 mole % N-doped TiO_2 NPs is nearly equal to that of bare TiO_2 NPs, which is similar with the crystallite size obtained from XRD. Further observation by SAED Figure 5(d) and in Figure 5(h) confirmed that the NPs are well crystalline in nature with tetragonal anatase structure. Figure 5(b and (f)) shows the lattice fringes of the material with inter planar spacing d spacing 0.25 and 0.26 nm matches well (101) plane of anatase TiO_2 crystal structure [3,19]

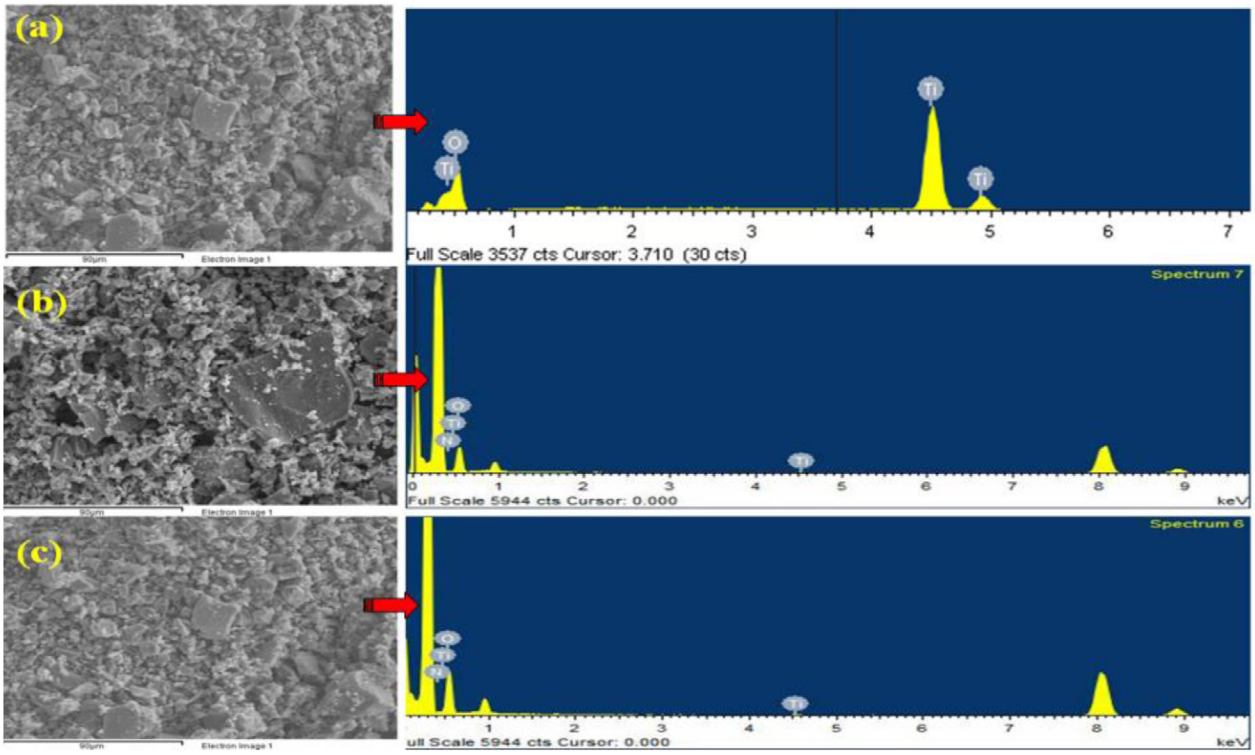

Figure 4. Elemental composition of (a) bare TiO_2, (b) 1% N, and (c) 5% N-doped TiO_2 NPs and the representative patterns of EDAX.

2.6. UV–Visible Diffuse Reflectance Spectroscopy (UV-Visible DRS)

UV-Visible diffused reflectance absorption spectra of all the prepared samples have been measured to understand the optical response and band gap energies of the synthesized materials. **Figure 6**a shows the UV-Visible DRS (absorption mode) spectra of bare TiO_2 NPs shows the optical absorption edge in the wavelength region between 250 and 390 nm,[20] while compared to N-doped TiO_2 (1, 3, and 5 mole% N) shows the shifting its

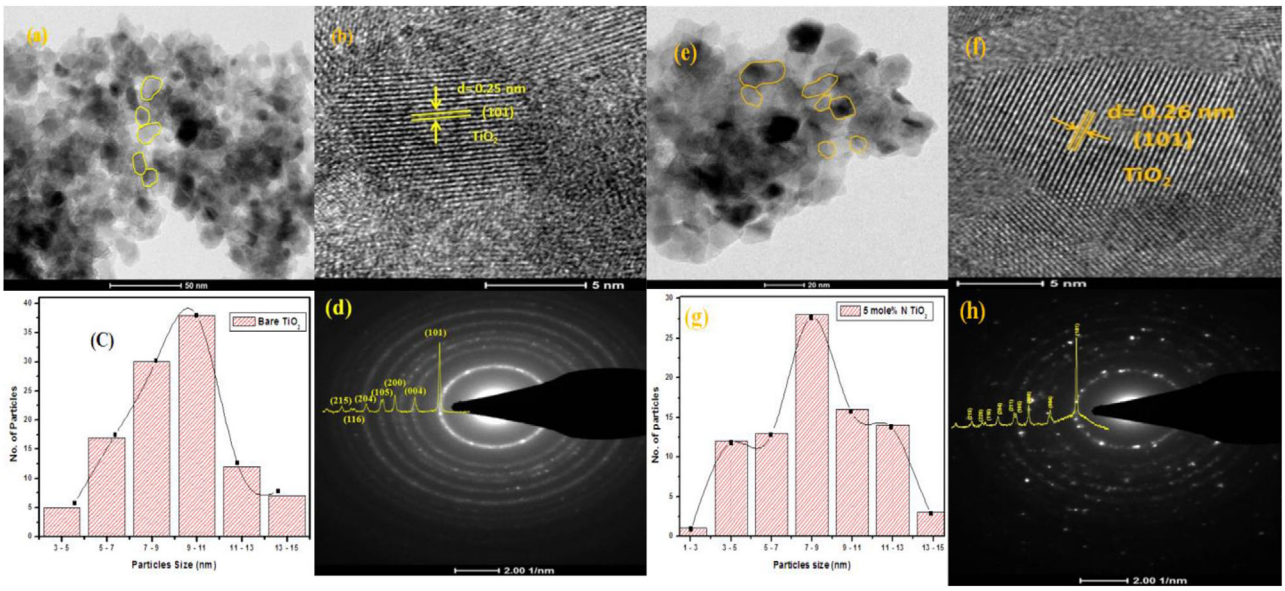

Figure 5. (a, b, c, d) shows the TEM, high-resolution TEM (HR-TEM), Histogram of particle size and selected area electron diffraction (SAED) pattern for bare TiO_2 and e, f, g, h) shows the TEM, High-resolution TEM (HR-TEM), Histogram of particle size and selected area electron diffraction (SAED) pattern for 5 mole% N-doped TiO_2.

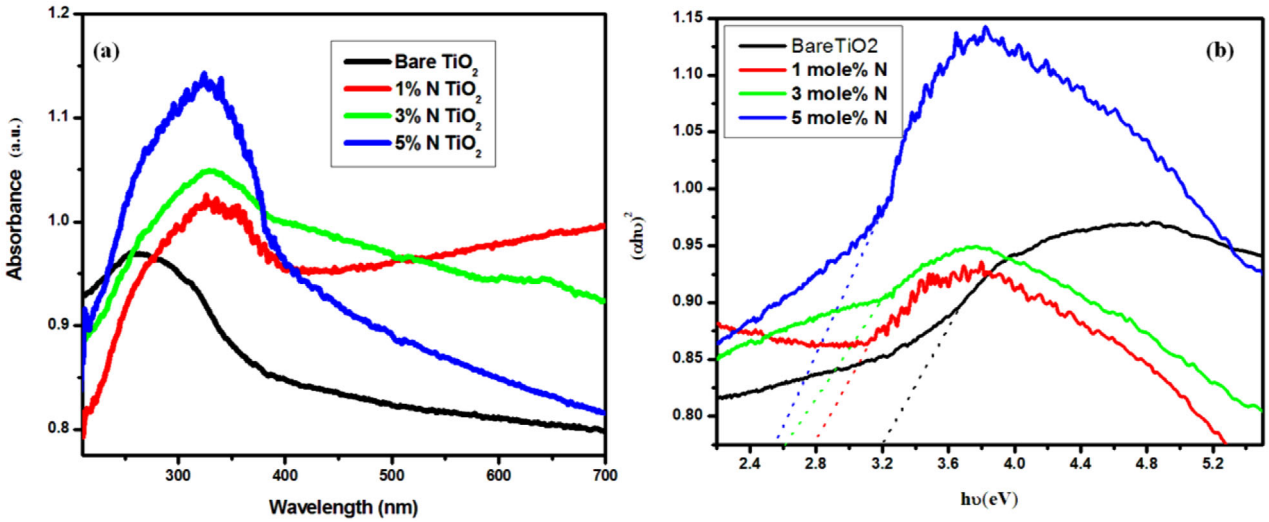

Figure 6. a) UV-Visible DRS (absorption mode) spectra of bare TiO_2 and 1, 3, and 5 mole % N doped TiO_2 NPs and (b) Tauc plot $(\alpha h\upsilon)^2$ as a function of photon energy ($h\upsilon$) of TiO_2 and N doped TiO_2 NPs with 1, 3, and 5 mole % Fe.

absorption edge from UV to visible region, indicates doping of N in the TiO_2 lattice.[21] As the mole% of N increases in the TiO_2, the visible absorption edge shifted towards higher absorbance as well as higher wavelength region; this is reflected through decrease in the optical band gap.[22] The N-doped TiO_2 samples show stronger absorption edge in the range of wavelengths from 400 to 530 nm compared with bare TiO_2.[23,24] This is attributed to isolated levels of N-2p orbitals in the band gap of TiO_2 and hence results light yellow color of doped TiO_2 with doping of nitrogen up to 5.0 mol%.[25]The optical energy band gap of the N-doped TiO_2 was determined by plotting the Tauc plot $(\alpha h\upsilon)^2$ as a function of photon energy ($h\upsilon$) and fixed from the intercept tangent to the x-axis [22] and presented in Figure 6(b). The energy band gap decreases from 3.2 to 2.5 eV as the doping of mole % of N increases as 1, 3, and 5 mole%. The doping of nitrogen in the TiO_2 lattice, the band gap is lowered to 2.8 eV for 1 mole% N, further reduced to 2.6 eV for 3 mole% N, and 2.5 eV for 5 mole% N doping in TiO_2. This absorption enhancement with decrease in band gap in the visible region can be assigned to the formation of dopant level nearer the valance band.[26] The decrease in the optical energy band gap of the N doped TiO_2 NPs, leads to increase in optical absorption.

3. Conclusions

Astringent morphology control in the synthesis of doped anatase crystal structure is considerably challenging because of the intrinsic properties of the anatase polymorph. In this study, a novel dopant, ethylenediaminetetraacetic acid (EDTA), was introduced to develop N-doped anatase crystal structure. N-doped TiO_2 NPs less than 11.85 nm were obtained, which are consistent with the FESEM and HR-TEM micrographs. By FT-IR and EDAX measurements, the presence of nitrogen into the N-doped TiO_2 structure was confirmed. Also, EDAX analysis showed the presence of impurities related to Ti^{4+} states. These impurities play a fundamental role in the optical activities of the N–doped TiO_2 by introducing localized states within the bandgap energy of the N-doped TiO_2. The enhanced optical activity of the N-doped TiO_2 was assessed under irradiation of UV and visible light.

4. Experimental Section

Materials: Nanocrystalline N-doped TiO_2 was synthesized by using the sol-gel technique. In this work, analytical grade titanium(IV)tetraisopropoxide (TTIP) $(TiOCH(CH_3)_{24}$ 97% Sigma Aldrich (AR)), Ethylenediaminetetraacetic acid (EDTA) $(C_{10}H_{16}N_2O_8$, Thomas Baker (LR)), Oleic acid $(C_{18}H_{34}O_2$, Research Lab (LR)), ammonia $(NH_3$, Thomas Baker (LR)) and absolute ethyl alcohol (C_2H_5OH, Research Lab (LR)) were used for the synthesis.

Synthesis of N-Doped TiO_2 NPs: Optimum compositions (0.0, 1, 3, and 5 mole %) of N-doped TiO_2 NPs were prepared by sol-gel method at room temperature. 5 mL oleic acid was taken in a 250 mL round-bottom flask. The content was stirred at 120°C for 10 min followed by the addition of 10 mL TTIP and 200 mL distilled water (DW); white precipitate of titanium hydroxide was formed. The content was stirred at room temperature for 1 h. Then, the content was filtered and re-slurred in 200 mL DW and the pH of the solution was adjusted to 10 by using an ammonia solution. After that, the content was stirred at 60°C for 3 h. The stoichiometric quantity of ethylenediaminetetraacetic acid (EDTA) $(C_{10}H_{16}N_2O_8)$ was added into the above solution. The content was again stirred for 3 h at 60°C. Then, the content was filtered and washed with 50 mL DW and 10 mL ethyl alcohol. After that, the residue was dried at 100°C and annealed in air at 500°C for 5 h. After annealing, the residue resulted in the off-white colored N-doped TiO_2 NPs.

Characterization: The prepared powder samples were characterized by powder XRD. XRD data of the samples were collected in the 2θ range of 10^0 – 90^0 in step scan mode at a rate of 0.2^0 min^{-1} using ULTIMA IV, Rigaku Corporation, Japan, diffractometer with source Cu Kα (Kα1 = 1.5406 and Kα1 = 1.5444 Å) radiation. Nicolet iS10, Thermo Scientific, USA FTIR spectrometer was used to record FTIR spectra of the NPs in the range of 400–4000 cm^{-1} with the transmission mode. The surface morphology of samples was investigated by using FE-SEM Hitachi S-4800 system with EDAX analysis was performed to determine the elemental composition of the samples. A JEOL JEM2100F field emission gun-transmission electron microscope (HR-TEM 200kV) operating at 200 kV with resolution (Point: 0.19 nm Line: 0.1 nm) and magnification (50X – 1.5 X) was employed for generating HR-TEM image of the NPs. UV–Visible

diffuse reflectance spectra of all the samples were recorded in the range of 200 –800 nm, using an ELICO – SL159 UV–Visible spectrometer.

Acknowledgements

The authors deeply acknowledges the Dr. Babasaheb Ambedkar Marathwada University, Aurangabad, for providing grants for the MRP. The authors also acknowledge the Principal, Ramkrishna Paramhansa Mahavidyalaya, Osmanabad, for providing the research facilities.

Conflict of Interest

The authors declare no conflict of interest.

Data Availability Statement

The data that support the findings of this study are available on request from the corresponding author. The data are not publicly available due to privacy or ethical restrictions.

Keywords

anatase, band gap, doping, heterogeneous catalyst, sol-gel method, visible light

Received: April 2, 2021
Revised: May 10, 2021

[1] N. Bayat, V. R. Lopes, J. Schölermann, L. D. Jensen, S. Ristobal, *Biomaterials* **2015**, *63*, 1.
[2] L. Chu, M. Li, P. Cui, Y. Jiang, Z. Wan, S. Dou, *Energy Environ. Focus.* **2014**, *3*, 371.
[3] S. P. Kunde, K. G. Kanade, B. K. Karale, H. N. Akolkar, S. S. Arbuj, P. V. Randhavane, S. T. Shinde, M. H. Shaikh, A. K. Kulkarni, *RSC Adv.* **2020**, *10*, 26997.
[4] M. Yadav, N. D. Thorat, M. M. Yallapu, T. Syed, J. Kim, *J. Mater. Chem. B* **2017**, *5*, 1461.
[5] S. M. Gupta, M. Tripathi, *Chin. Sci. Bull.* **2011**, *56*, 1639.
[6] G. Qin, Z. Sun, Q. Wu, L. Lin, M. Liang, S. Xue, *J. Hazard. Mater.* **2011**, *192*, 599.
[7] S. W. Verbruggen, M. Keulemans, M. Filippousi, D. Flahaut, G. Van Tendeloo, S. Lacombe, J. A. Martens, S. Lenaerts, *Appl. Catal. B Environ.* **2014**, *156–157*, 116.
[8] E. A. Kozlova, A. Y. Kurenkova, V. S. Semeykina, E. V. Parkhomchuk, S. V. Cherepanova, E. Y. Gerasimov, A. A. Saraev, V. V. Kaichev, V. N. Parmon, *ChemCatChem.* **2015**, *7*, 4108.
[9] H. M. Yadav, S. V. Otari, V. B. Koli, S. S. Mali, C. K. Hong, S. H. Pawar, S. D. Delekar, *J. Photochem. Photobiol. A Chem.* **2014**, *280*, 32
[10] H. M. Yadav, J. S. Kim, S. H. Pawar, *Korean J. Chem. Eng.* **2016**, *33*, 1989.
[11] J. Xu, F. Wang, W. Liu, W. Cao, *Int. J. Photoenergy* **2013**, https://doi.org/10.1155/2013/616139.
[12] S. D. Delekar, H. M. Yadav, S. N. Achary, S. S. Meena, S. H. Pawar, *Appl. Surf. Sci.* **2012**, *263*, 536.
[13] A. Sanchez-Martinez, O. Ceballos-Sanchez, C. Koop-Santa, E. R. López-Mena, E. Orozco-Guareño, M. García-Guaderrama, *Ceram. Int.* **2017**, S02728842, 32851-1.
[14] K. Nagaveni, M. S. Hegde, N. Ravishankar, G. N. Subbanna, G. Madras, *Langmuir* **2004**, *20*, 2900.
[15] H. Luo, S. Dimitrov, M. Daboczi, Ji-S Kim, Q. Guo, Y. Fang, M. -. A. Stoeckel, P. Samorì, O. Fenwick, A. B. J. Sobrido, X. Wang, M. -. M. Titirici, *ACS Appl. Nano Mater.* **2020**, *3*, 3371.
[16] M. L. Mane, S. E. Shirsath, V. N. Dhage, K. M. Jadhav, *Nucl. Inst. Meth. Phys. Res. B* **2011**, *269*, 2026.
[17] S. Bae, H. Kim, Y. Lee, X. Xu, J. Park, Y. Zheng, J. Balakrishnan, T. Lei, H. RiKim, Y. Song, Y. Kim, K. S. Kim, B. Özyilmaz, J. Ahn, B. Hong, S. Iijima, *Nat. Nanotechnol.* **2010**, *5*, 574.
[18] M. Landmann, E. Rauls, W. G. Schmidt, *J. Phys. Condens. Matter* **2012**, *24*, 195.
[19] S. B. Deshmukh, D. V. Mane, M. G. Bhosale, M. L. Mane, J. D. Ambekar, *High Technol. Lett.* **2020**, *26*, 159.
[20] T. L. Thompson, J. T. Yates, *Chem. Rev.* **2006**, *106*, 4428.
[21] S. Shaw, E. Jayatilleke, *Alcohol* **1992**, *9*, 363.
[22] G. Cheng, M. S. Akhtar, O. - B. Yang, F. J. Stadler, *ACS Appl. Mater. Interfaces* **2013**, *5*, 6635.
[23] V. C. Stengl, D. Popelková, P. Vláčil, *J. Phy. Chem.C* **2011**, *115*, 25209.
[24] J. T. Robinson, S. M. Tabakman, Y. Liang, H. Wang, H. Sanchez Casalongue, D. Vinh, H. Dai, *J. Am. Chem. Soc.* **2011**, *133*, 6825.
[25] Y. Zhou, Y. Liu, P. Liu, W. Zhang, M. Xing, J. Zhang, *Appl. Catal. B Environ.* **2015**, 170e171 66e73.
[26] T. Umebayashi, T. Yamaki, H. Itoh, K. Asai, *J. Phys. Chem. Solids* **2002**, *63*, 1909.